Wave-equation Migration Velocity Analysis

Biondo Biondi and Paul Sava , Stanford University*

SUMMARY

We introduce a new wave-equation method of Migration Velocity Analysis. The method is based on the linear relation that can be established between a perturbation in the migrated image and the generating perturbation in the slowness function. Our method iteratively updates the slowness function to account for improvements in the focusing quality of the migrated image. As a wave-equation method, our MVA is robust and generates smooth slowness functions without model regularization. We also show that our method has the potential to exploit the power of residual prestack migration.

INTRODUCTION

Seismic imaging is a two-step process: velocity estimation and migration. As the velocity function becomes more complex, the two steps become more and more dependent on each other. In complex depth imaging problems, velocity estimation and migration are applied iteratively in a loop. To assure that this iterative imaging process converges to a satisfactory model, it is crucial that the migration and the velocity estimation are consistent with each other.

Kirchhoff migration often fails in complex areas, such as sub-salt, because the wavefield is severely distorted by lateral velocity variations and thus complex multipathing occurs. As the shortcomings of Kirchhoff migration have become apparent (O'Brien and Etgen, 1998), there has been a renewal of interest in wave-equation migration and the development of computationally efficient 3-D prestack depth migration methods based on the wave equation (Biondi and Palacharla, 1996; Biondi, 1997; Mosher et al., 1997). However, there has been no corresponding progress in the development of Migration Velocity Analysis (MVA) methods that can be used in conjunction with wave-equation migration. We present a method that aims at filling this gap and that, at least in principle, can be used in conjunction with any downward-continuation migration method. In particular, we have been applying our new methodology to downward continuation based on the Double Square Root equation in 2-D (Yilmaz, 1979; Claerbout, 1985; Popovici, 1996) and on common-azimuth continuation in 3-D (Biondi and Palacharla, 1996).

As for migration, wave-equation MVA is intrinsically more robust than ray-based MVA because it avoids the well-known problems that rays encounter when the velocity model is complex and has sharp boundaries. The transmission component of finite-frequency wave propagation is mostly sensitive to the smooth variations in the velocity model. Consequently, wave-equation MVA produces smooth velocity updates and is thus stable. In most cases, no smoothing constraints are needed to assure stability in the inversion. On the contrary, ray-based methods require strong smoothing constraints to avoid quick divergence.

Our method is closer to conventional MVA than other wave-equation methods that have been proposed to estimate the background velocity model (Noble et al., 1991; Bunks et al., 1995; Fogues et al., 1998) because it tries to maximize the quality of the migrated image instead of trying to match the recorded data. In this respect, our method is related to Differential Semblance Optimization (Symes and Carazzone, 1991) and Multiple Migration Fitting (Chavent and Jacewitz, 1995). However, with respect to these two methods, our method has the advantage of exploiting the power of residual prestack migration to speed up the convergence.

ESTIMATION ALGORITHM

We estimate velocity by iteratively migrating the prestack data and looping over the following steps:

1. Downward continuation with current velocity
2. Extraction of Common-Image Gathers from prestack wavefield (Prucha et al., 1999)
3. Residual prestack migration of Common-Image Gathers
4. Estimation of image perturbation from residual prestack migration results
5. Estimation of velocity perturbation from image perturbations

The core technical element of the method is the estimation of velocity perturbations from image perturbations. The next section presents the linear theory that enables us to achieve this goal.

LINEAR THEORY

In migration by downward continuation (Figure 1), data measured at the surface (D) is recursively pushed down in depth to generate the complete wavefield (U). Downward continuation requires us to make an assumption of the slowness field (S). Once the wavefield is known, we can apply the imaging condition which gives us the wavefield at time zero, or in the other words, the image or reflectivity map at the moment the reflectors explode (R).

In the presence of the background wavefield (U), a perturbation in slowness (ΔS) will generate a scattered wavefield (ΔW), which can, by the same method as the background field, be downward continued (ΔU) and imaged (ΔR) (Figure 1).

We can now take the perturbation in image (ΔR) and apply the adjoint operation. This will lead to an adjoint perturbation in wavefield (ΔU^*), an adjoint scattered field (ΔW^*), and eventually to an adjoint perturbation in slowness (ΔS^*) (Figure 1). Considering a first order Born relation between the perturbation in slowness and the scattered wavefield, we can establish a direct linear relation between the perturbation in image (ΔR) and the perturbation in slowness (ΔS). It follows that if we can obtain a better focused image, we can iteratively invert for the perturbation in slowness that generates the better focusing. This is the foundation of our wave-equation MVA method.

In the following sections we will briefly present the mathematical relations on which our method is based.

Background field: Forward operator

Migration by downward continuation, in post-stack or pre-stack, is done in two steps: the first step is to downward continue the data (D) measured at the surface, and the second is to apply the imaging condition, that is to extract the wavefield at time $t = 0$, or the image (R), at the moment the reflectors explode (Claerbout, 1985).

1. Downward continuation

   The first step of migration consists of downward continuation of the wavefield measured at the surface (a.k.a. the data), which is done by the recursive application of the equation:

   $$u_0^{z+1} = T^z u_0^z \tag{1}$$

   initialized by the wavefield at the surface:

   $$u_0^1 = f \cdot d \tag{2}$$

   where:

Wave-equation MVA

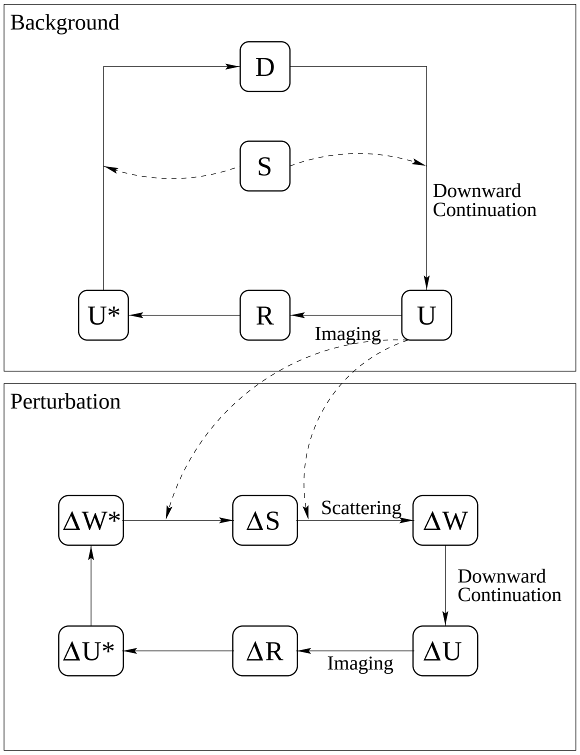

Figure 1: Processing chart.

- $u_0^z(\omega)$ is the wavefield $u_0(\omega)$ at depth z.
- $u_0^1(\omega)$ is the wavefield $u_0(\omega)$ at the surface.
- $T^z(\omega, s_0)$ is the downward continuation operator at depth z.
- $d(\omega)$ is the data, i.e. the wavefield at the surface.
- $f(\omega)$ is a frequency dependent scale factor for the data.

2. Imaging

   The second step of the migration by downward continuation is imaging. In the exploding reflector concept, the image is found by selecting the wavefield at time $t = 0$, or equivalently, by summing over the frequencies (ω):

$$r_0^z = \sum_1^{N_\omega} u_0^z(\omega) \tag{3}$$

   where:

   - r_0^z is the image (reflectivity) corresponding to a given depth level (z).

Perturbation field: Forward Operator
If we perturb the velocity model we introduce a perturbation in the wavefield. In other words, the perturbation in slowness has generated a secondary scattered wavefield.

1. Scattering and Downward Continuation

   If we consider the perturbation in wavefield at the surface, we can recursively downward continue it, adding at every depth step the scattered wavefield:

$$\Delta u^{z+1} = T^z \Delta u^z + \Delta v^{z+1} \tag{4}$$

   where

   - $\Delta u^z(\omega)$ is the perturbation in the wavefield generated by the perturbation in velocity, and downward continued from the surface.
   - $\Delta v^{z+1}(\omega)$ represents the scattered wavefield caused at depth level $z+1$ by the perturbation in velocity from the depth level z.

   The first order Born approximation of the scattered wavefield can be written as:

$$\Delta v^{z+1} = T^z G^z u_0^z \Delta s^z \tag{5}$$

   where:

   - $G^z(\omega, s_0)$ is the scattering operator at depth z.
   - $\Delta s^z(\omega)$ is the perturbation in slowness at depth z.
   - $u_0^z(\omega)$ is the background wavefield at depth z.

   If we introduce the equation (5) in (4) we obtain that:

$$\Delta u^{z+1} = T^z \left[\Delta u^z + G^z u_0^z \Delta s^z \right] \tag{6}$$

2. Imaging

   As for the background image, the perturbation in image (Δr^z), caused by the perturbation in slowness, is obtained by a summation over all the frequencies (ω):

$$\Delta r^z = \sum_1^{N_\omega} \Delta u^z(\omega) \tag{7}$$

The equations (6) and (7) establish a linear relation between the perturbation in slowness (Δs^z) and the perturbation in image (Δr^z). We can use this linear relation in an iterative algorithm to invert for the perturbation in slowness from the perturbation in image.

Perturbation field: Adjoint Operator
In the adjoint operation, we begin by upward propagating the perturbation in wavefield at depth:

$$\Delta u^z = T^{z*} \Delta u^{z+1} + \Delta r^z \tag{8}$$

where

- T^{z*} is the upward continuation operator at depth z.

We can then obtain the perturbation in slowness from the perturbation in wavefield by applying the adjoint of the scattering operator:

$$\Delta s^z = u_0^{z*} G^{z*} \left[T^{z*} \Delta u^{z+1} - \Delta u^z \right] \tag{9}$$

The equations (6) and (7) for the forward operator, and the equations (8) and (9) for the adjoint operator, express the linear relation established between the perturbation in slowness (ΔS) and the perturbation in image (ΔR).

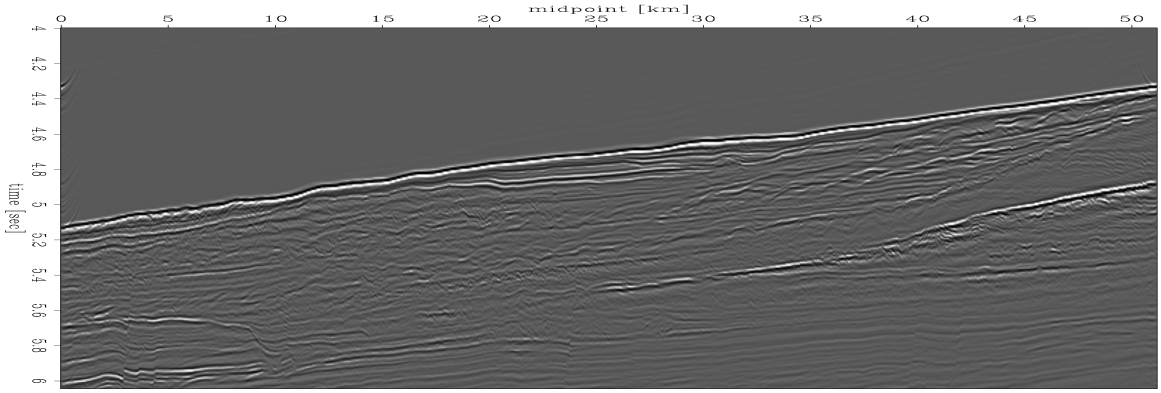

Figure 2: Original image.

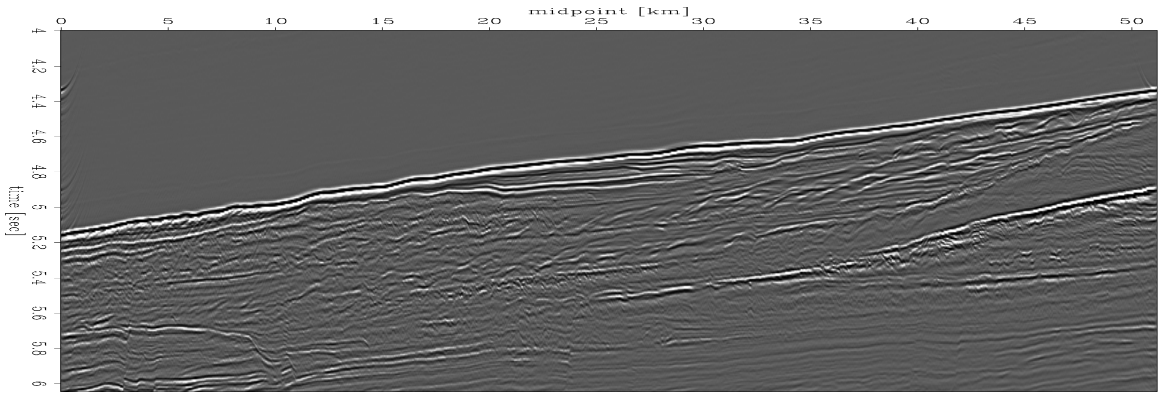

Figure 3: Better focused image after residual migration.

EXAMPLE

In the first part of our example we will concentrate on improving the focusing of the image. To achieve an enhanced focusing, we used Stolt residual migration in the prestack domain (Stolt, 1996; Sava, 1999). Another alternative to obtain a better focusing would be to use velocity continuation (Fomel, 1997). The dataset is part of a gas-hydrate study, and was recorded at the Blake Outer Ridge, offshore Florida and Georgia (Ecker, 1998).

Figure (2) shows the image obtained with a starting velocity model, while Figure (3) shows an image obtained by applying residual migration to the original. The second image is clearly better focused than the original, and therefore appears more energetic.

We can take the difference between the two images, (2) and (3), to be the perturbation in image (ΔR), and use it to invert for the slowness model that generates the better focus.

For the second part of our example, we have constructed a model inspired by the sections in Figures (2) and (3). The goal is to convert the differences in focusing between the two images (perturbation in image) into a better slowness model (i.e. to find the perturbation in slowness).

Figure (4) represents the background slowness model (S). We will use this model to generate the background wavefield (U), and the background image (R) from the synthetic data at the surface (D).

Figure (5) contains the perturbation in slowness (ΔS). We will use this model to generate the scattered wavefield (ΔW), the perturbation wavefield (ΔU), and the perturbation in image (ΔR). We will start the inversion by assuming zero perturbation in slowness.

Figure (6) represents the perturbation in slowness obtained at the first iteration. For now, only a small perturbation in slowness is obtained, though it is not totally concentrated at the right location. Part of the energy of the section is spread, for example at about midpoint $2.2 - 2.4$km and at depth $1.3 - 1.4$km. This artifact is the result of the still imperfect definition of the slowness anomaly, and possibly it is also due to the proximity of the edge.

By the 20th iteration (Figure 7), the perturbation in slowness is much better shaped, and the artifact at depth is much weaker. Also, the absolute magnitude of the anomaly is getting very close to the correct value: $s_{max} = 0.088$s/km for the original, and $s_{max} = 0.084$s/km for the inversion at iteration 20.

CONCLUSION

We have presented a recursive wave-equation Migration Velocity Analysis method operating in the image domain. Our method is based on the linearization of the downward continuation operator that relates perturbations in slowness to perturbations in image. The fundamental idea is to improve the quality of the slowness function by optimizing the focusing of the migrated image.

The iterative method is very stable and accurate when applied to a synthetic dataset. It also converges to the solution without the need for any regularization of the slowness model. We are currently in the process of applying the method to the real seismic dataset used as an example in this expanded abstract.

REFERENCES

Biondi, B., and Palacharla, G., 1996, 3-D prestack migration of common-azimuth data: Geophysics, **61**, 1822–1832.

Biondi, B., 1997, Azimuth moveout + coomon-azimuth migration: Cost-effective prestack depth imaging of marine data: 67th Annual Internat. Mtg., Soc. Expl. Geophys., Expanded Abstracts, 1375–1378.

Bunks, C., Saleck, F. M., Zaleski, S., and Chavent, G., 1995, Multiscale seismic waveform inversion: Geophysics, **60**, no. 5, 1457–1473.

Chavent, G., and Jacewitz, C. A., 1995, Determination of background velocities by multiple migration fitting: Geophysics, **60**, no. 2, 476–490.

Claerbout, J. F., 1985, Imaging the Earth's Interior: Blackwell Scientific Publications.

Ecker, C., 1998, Seismic characterization of gas hydrates structures: Ph.D. thesis, Stanford University.

Fogues, E., Scala, E., and Pratt, R. G., 1998, High resolution velocity estimation from refraction and reflection data: 68th Annual Internat. Mtg., Soc. Expl. Geophys., Expanded Abstracts, 1211–1214.

Fomel, S., 1997, Velocity continuation and the anatomy of residual prestack migration: 67th Ann. Internat. Meeting, Soc. Expl. Geophys., 1762–1765.

Mosher, C. C., Foster, D. J., and Hassanzadeh, S., 1997, Common angle imaging with offset plane waves: 67th Annual Internat. Mtg., Soc. Expl. Geophys., Expanded Abstracts, 1379–1382.

Noble, M., Lindgren, J., and Tarantola, A., 1991, Large-sized, nonlinear inversion of a marine data set: Retrieving the source, the background velocity and the impedance contrasts: 61th Annual Internat. Mtg., Soc. Expl. Geophys., Expanded Abstracts, 893–896.

O'Brien, M. J., and Etgen, J. T., 1998, Wavefield imaging of complex structures with sparse point-receiver data: 68th Annual Internat. Mtg., Soc. Expl. Geophys., Expanded Abstracts, 1365–1368.

Popovici, A. M., 1996, Short note - prestack migration by split-step DSR: Geophysics, **61**, no. 05, 1412–1416.

Prucha, M., Biondi, B., and Symes, W., 1999, Angle-domain common image gathers by wave-equation migration: 69th Annual Internat. Mtg., Soc. Expl. Geophys., Expanded Abstracts, submitted.

Sava, P., 1999, Short note - On Stolt prestack residual migration: SEP-Report, **100**.

Stolt, R. H., 1996, Short note - a prestack residual time migration operator: Geophysics, **61**, no. 02, 605–607.

Symes, W. W., and Carazzone, J. J., 1991, Velocity inversion by differential semblance optimization: Geophysics, **56**, no. 5, 654–663.

Yilmaz, O., 1979, Prestack partial migration: Ph.D. thesis, Stanford University.

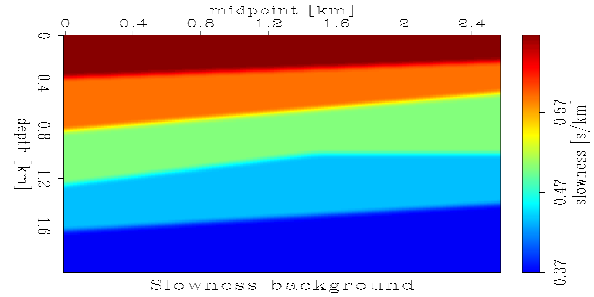

Figure 4: Background slowness (S).

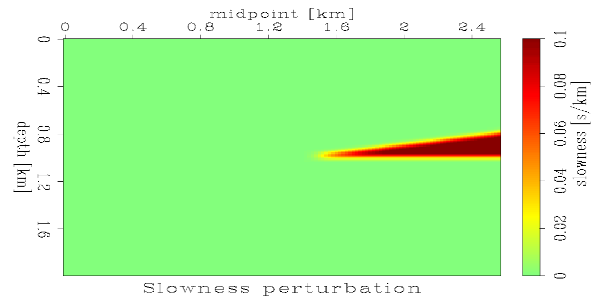

Figure 5: Perturbation in slowness (ΔS).

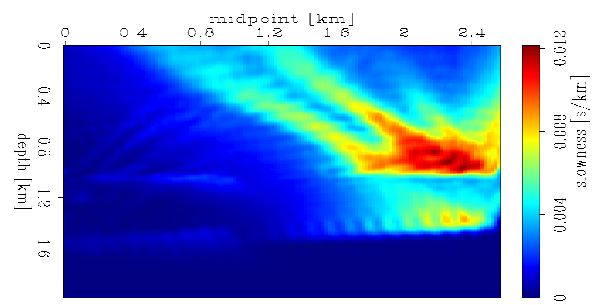

Figure 6: Recovered perturbation at iteration 1.

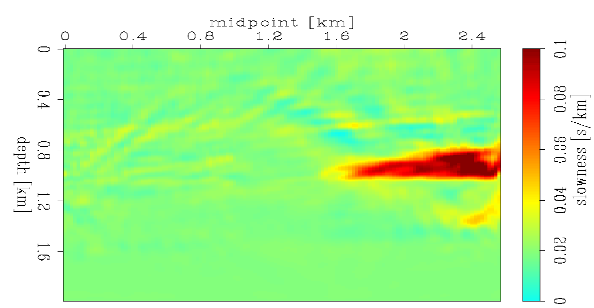

Figure 7: Recovered perturbation at iteration 20.